Relationship of Polycyclic Aromatic Hydrocarbons with Oxy (Quinone) and Nitro Derivatives During Air Mass Transport

Harrison, Roy; Alam, Mohammed; Dang, Juan; Ismail, I.M.; Basahi, J; Alghamdi, Mansour A.; Hassan, I.A.; Khoder, M.

DOI:
10.1016/j.scitotenv.2016.08.030

Document Version
Peer reviewed version

Citation for published version (Harvard):
Harrison, R, Alam, M, Dang, J, Ismail, IM, Basahi, J, Alghamdi, MA, Hassan, IA & Khoder, M 2016, 'Relationship of Polycyclic Aromatic Hydrocarbons with Oxy (Quinone) and Nitro Derivatives During Air Mass Transport', *Science of the Total Environment*, vol. 572, pp. 1175-1183. https://doi.org/10.1016/j.scitotenv.2016.08.030

RELATIONSHIP OF POLYCYCLIC AROMATIC HYDROCARBONS WITH OXY (QUINONE) AND NITRO DERIVATIVES DURING AIR MASS TRANSPORT

Roy M. Harrison[1,2,3*], Mohammed S. Alam[1], Juan Dang[1‡], I.M. Ismail[2], J. Basahi[2], Mansour A. Alghamdi[3] I.A. Hassan[2,4] and M. Khoder[2,3]

[1]School of Geography, Earth and Environmental Sciences University of Birmingham, Edgbaston, Birmingham, B15 2TT United Kingdom

[2]Center of Excellence in Environmental Studies, King Abdulaziz University, Jeddah, 21589, Saudi Arabia

[3]Department of Environmental Sciences, Faculty of Meteorology Environment and Arid Land Agriculture, King Abdulaziz University Jeddah, Saudi Arabia

[4]Faculty of Science, Alexandria University 21526 El Shatby, Alexandria, Egypt

[‡] Also at: Environment Research Institute, Shandong University, Jinan 250100, P.R. China
[*] To whom correspondence should be addressed
Tele: +44 121 414 3494; Fax: +44 121 414 3708; Email: r.m.harrison@bham.ac.uk

ABSTRACT

Airborne concentrations of Polycyclic Aromatic Hydrocarbons (PAH), quinone and nitro derivatives have been measured at three sites on the coast of Saudi Arabia to the north of the city of Jeddah. The PAH show a general reduction in concentrations from northwest to southeast, consistent with a source from a petrochemical works to the northwest of the sampling sites. In comparison, the concentrations of quinones show little variation between the sampling sites consistent with these being predominantly longer lived secondary pollutants formed from PAH oxidation. The nitro-PAH show a gradient in concentrations similar to but smaller than that for the PAH suggesting a balance between atmospheric formation and removal by photolysis. The 2-nitrofluoranthene:1-nitropyrene ratio increases from north to south, consistent with atmospheric chemical formation of the former compound, while the ratio of 2-nitrofluoranthene:2-nitropyrene is consistent with hydroxyl radical as the dominant reactant. An investigation of the changes in PAH congener ratios during air mass transport along the Red Sea coast shows consistency with reaction with a relatively low concentration of hydroxyl radical only for the day with the highest concentrations. It is concluded that while PAH degradation is occurring by chemical reaction, emissions from other locations along the air mass trajectory are most probably also leading to changes in congener ratios.

Keywords: Polycyclic aromatic hydrocarbons; quinones; nitro-PAH; atmospheric concentrations; chemical reactions.

1. INTRODUCTION

Polycyclic aromatic hydrocarbons (PAH) are a group of compounds emitted widely to the atmosphere from pyrolytic and petrogenic sources such as hydrocarbon fuel combustion and evaporation (Ravindra et al., 2008; Harrison et al., 1996). Their atmospheric concentrations are measured both in national networks and in research studies in many parts of the world. Some members of the PAH group of compounds (congeners) are known human carcinogens and the World Health Organization has determined an exposure-response function for cancer of the lung as a result of PAH exposure, and has also reviewed other non-cancer effects upon human health (WHO, 2010). The European Union has set a target value of 1 ng m^{-3} of benzo(a)pyrene as an aspirational limit to minimise adverse effects upon public health.

PAH are reactive compounds and are oxidised in the atmosphere with lifetimes typically from hours to days (Keyte et al., 2013). Amongst the first products of oxidation are oxy-derivatives, typically quinones, and nitro derivatives. Far less is known about the carcinogenic activity of the derivatives than for the PAH, but PAH quinones have been linked with reactive oxygen species (Verma et al., 2015) and oxidative stress (Li et al., 2003), an important mechanism in the development of human disease, and both quinones and nitro-PAH are potent *in vitro* mutagens with a consequent potential to cause cancer or teratogenesis (Durant et al., 1996; Pederson and Siak, 1981).

Keyte et al. (2013) have reviewed the chemical reactivity, including mechanisms of PAH oxidation and their potential for long-range transport. Walgraeve et al. (2010) reviewed the published data describing oxygenated PAH in the atmosphere, including measurements of ketones, carboxaldehydes, diones and quinones. Noting the relative scarcity of quinone data, Delgado-Saborit et al. (2013) report measurements of 14 PAH quinones in Standard Reference Material (Urban Dust) SRM1649a and SRM1649b, and in the ambient air. They compare their ambient air concentration data with that from 14 other published studies. Other than for anthraquinone and

7,12-benzo(a)anthracene quinone which are reported by most studies, the majority of compounds are reported only by a sub-set of studies. Furthermore, Delgado-Saborit et al. (2013) studied the partition of quinones between the condensed and vapour phases. They found that, as for PAH, molecular weight is a good predictor of partitioning and a transition occurs in the region of molecular weight 200 to 250 from a presence predominantly in the vapour phase, to one which is mainly particle-associated, with the 50% point at molecular weight 230-240, when average air temperatures were in the range of 1-4ºC. Albinet et al., 2008 investigated the partitioning of PAH, oxy-PAH and nitro-PAH during the summer and winter seasons and noted that the partitioning of oxy-PAH and nitro-PAH were significantly different in both seasons. The 50% point at which compounds were present in the vapour and condensed phase increased in the summer from a molecular weight of 180-190 to 200-210 for oxy-PAH and 190-200 to 210-220 for nitro-PAH, confirming that temperature may have an influence in the partitioning. Data for nitro-PAH in the atmosphere are scarce in the literature, with very few studies reporting concentrations of a few compounds (e.g. Albinet et al., 2007; Ringuet et al., 2012; Souza et al., 2014; Dimashki et al., 2000).

In this study, concentrations of PAH, quinones and nitro-derivatives have been measured during summer and winter periods at three sites in Saudi Arabia and the concentration data and inter-relations between compounds are reported in this paper. The spatial distribution of the PAH has been discussed in an earlier paper (Harrison et al., 2016), where it was concluded that the emissions from the large petrochemical works at Yanbu to the northwest of Rayes could be responsible for the observed spatial distribution and congener profile of PAH.

2. AIR SAMPLING AND ANALYSIS

The air sampling sites and protocols used in this work have been reported by Harrison et al. (2016), and a map of the sampling locations appears in Figure 1. Particulate and vapour forms of the PAH

and their derivatives were sampled separately onto quartz filters and a PUF substrate respectively using a Tisch "pesticide" sampler with a TSP inlet. Samples were collected over 24-hour periods, offset by 6 hours between samples, commencing at Rayes, with sampling 6 hours later at Rabegh and a further 6 hours later at Abhur.

Quartz filters were cleaned prior to use by heating at 400ºC, followed by storage in a sealed container. PUF substrates were cleared by ultrasonification in dichloromethane (200 mL) at 20ºC for 30 minutes. These were stored in sealed bags in a -18ºC freezer. After use in the field, filters and PUF substrates were wrapped in cleaned aluminium foil, sealed in plastic bags and stored at -18ºC. The extraction, clean-up and preparation of samples prior to analysis incorporated a solid phase extraction step developed from methods described previously (Albinet et al., 2006; Cochran et al., 2012). Briefly, samples were spiked with a known amount of p-terphenyl-d14 (>99% purity, Greyhound Chromatography, Merseyside, UK) and 1-fluoro-7-nitrofluorene (>98% purity, Sigma-Aldrich Company Ltd., Gillingham, UK) as recovery standards for PAH and OPAH/NPAH, respectively. Filters were placed inside a glass flask and spiked with internal standard (IS) mixture (deuterated PAH, NPAH and OPAH compounds (>98% purity, Sigma-Aldrich Company Ltd., Gillingham, UK)). Approximately 15 mL DCM (HPLC grade, >98% purity, Fisher Scientific UK Ltd) was added and the flask was covered with aluminium foil to prevent any evaporative loss of analyte and/or standard. PUF substrates were placed and compressed inside a large glass beaker, spiked with IS mixture. Approximately 300 mL DCM was added to each PUF substrate.

Filters and PUF substrates were extracted by ultrasonication at 20°C for 30 minutes. Due to the larger volume of solvent used for PUF substrate extractions, samples were initially transferred to Turbovap apparatus (biotage Ltd, Uppsala, Sweden) and blown down under a gentle stream of nitrogen to reduce sample volume to approximately 5mL, prior to sample clean up. Extracted samples were passed through a Pasteur pipette containing 1g anhydrous sodium sulphate (Sigma-

Aldrich Company Ltd., Gillingham, UK), concentrated under a gentle stream of nitrogen to almost dryness and then made up to 1mL with hexane (HPLC grade, >98% purity, Fisher Scientific UK Ltd).

Sample extracts were then subject to a solid phase extraction step, based on the methodology described by Cochran et al., (2012). An aminopropyl solid phase extraction tube (Sigma-Aldrich Company Ltd., Gillingham, UK) was pre-eluted with 3x 1mL aliquots of DCM followed by the same measure of hexane. The sample was then passed through the column and target compounds were eluted by the sequential DCM/hexane solvent gradient (3 x 1mL) of 20/80%, 35/65%, 50/50%. This resulted in optimum recovery of PAH, NPAH and OPAH compounds in one sample extract to undergo analysis for PAH and OPAH/NPAH separately. Extracts were further reduced under nitrogen to almost dryness and made up to a final volume of 100 µL with nonane (HPLC grade, >98% purity, Fisher Scientific UK Ltd), ready for analysis.

Sixteen PAH, listed in Table 1 were analysed using Gas Chromatography (Agilent 6890) on a non-polar capillary column (Agilent HP-5MS, 30 m, 0.25 mm ID, 0.25 µm film thickness – 5% phenylpolysiloxane) coupled to a quadrupole mass spectrometer (Agilent 5973N). Detection limits lay below 1 pg m^{-3} for all compounds, and precision was 8 ± 4%, and accuracy (defined as the difference between the measured and true value as a percentage of the true value) was 6 ± 4% (Delgado-Saborit et al., 2010). Analysis of NIST SRM 1649b was used to quality assure the measurements.

Quinone and nitro-PAH compounds were analysed using Gas Chromatography (Agilent 6890W) on a Restek Rxi-PAH column (60 m, 0.25 mm ID, 0.1 µm film thickness) coupled to an Agilent 5973 MSD operated in negative ion chemical ionisation (NICI) and SIM mode, as in Alam et al., (2015). We demonstrated good agreement of our measurements with values reported for NIST SRM 1649b

153 (as in Delgado-Saborit et al., 2013). Some of the PUF substrates were found to be contaminated in
154 the high molecular weight (five to seven rings) region, making quantification uncertain.
155 Concentrations expressed are therefore only for the particle phase of these compounds, but the error
156 is likely to be no more than ca. 10% (Alghamdi et al., 2015; Delgado-Saborit et al., 2013).
157
158 As site details are important to the interpretation of these data, these are given below:
159
160 **Site C (Abhur) (21.7572ºN; 39.1147ºE)** is located in the grounds of a research institute on the Red
161 Sea coast to the west of major roads. It is in the northern suburbs of the major city of Jeddah
162 (population 5 million), with the King Abdulaziz international airport to the east (inland). The site is
163 approximately 130 km to the SE of Rabegh.
164
165 **Site D (Rabegh) (22.8122ºN; 39.0664ºE)** is a site located about 1 km from the residential areas of
166 this substantial city, which has appreciable local industry. The sampling site is ca. 500 metres east
167 of the coastal road. It is approximately 100 km SSE of Rayes.
168
169 **Site E (Rayes) (23.5756ºN; 38.6058ºE)** is a sparsely developed area with little road traffic and no
170 appreciable local sources. The sampling site is located about 950 metres inland (east) of the coastal
171 road, and 25-50 km SSE of the large industrial complex in the region of Yanbu.
172
173 ## 3. RESULTS AND DISCUSSION
174 Polycyclic aromatic hydrocarbons (PAH) are reactive in the atmosphere with lifetimes typically of a
175 few hours for the most reactive congeners, and a few days for the least. Ratios of compounds can
176 change dramatically during atmospheric transport as a result of differential reactivity. Alam et al.
177 (2013) have interpreted differences in concentration ratios between roadside and urban background
178 sites in terms of differential reactivity of congeners. Compounds of low reactivity showed only a

small elevation in concentration at the roadside site, while the more reactive compounds show larger ratios due to loss in the more aged air sampled at the background site. Using a similar approach, Alam et al. (2014) studied ratios between congeners measured in urban air, and those sampled in rural air. The urban/rural ratios were found to be greatest for the more reactive compounds, and in air masses which had aged most during atmospheric transport.

Concentrations of PAH measured in this study have been discussed by Harrison et al. (2015) and will not be considered further. The measured concentrations of the parent PAH, quinones and nitro-PAH appear in Table 1, and ranges of comparative data from the literature appear in Tables 2 and 3. There are large divergences between published studies seen in Tables 2 and 3 for the sampled compounds, which are seen clearly when individual studies are identified in Tables S1 and S2 (Supplementary Information). These may arise from strongly differing degrees of local pollution, or interferences in the analytical procedure. These are challenging trace analyses, and hence analytical artefacts are a very real possibility. However, the concentrations measured in our work (Table 1) appear broadly consistent with those published previously (Tables S1 and S2). The PAH concentrations have been discussed in relation to other published data by Harrison et al. (2016).

In addition to mean concentration, Table 1 includes the percentage particulate phase (%P). As is normally seen in PAH datasets, there is a strong trend of increasing percentage particulate phase with molecular weight, with three ring compounds being almost wholly vapour, while the compounds with five or more rings are predominantly particulate. This trend has been reported previously in samples collected in Jeddah, Saudi Arabia by Alghamdi et al. (2015). Similar behaviour is seen also in the quinones (as noted previously by Delgado-Saborit et al., 2013) and nitro-PAH (see Table 1).

3.1 Quinone: Parent PAH Ratios

Alam et al. (2014) also studied quinone:parent PAH ratios, finding a relationship to air mass age. In winter, ratios of phenanthraquinone to phenanthrene (PQ:PHE) in the UK were highest in the most aged air masses with origins in the arctic, with some values in the range 1.0-1.2, although some lower values were also present. In the less aged air from mainland Europe and the United Kingdom, ratios were lower, almost all falling below PQ/PHE = 0.4. In the present work, winter ratios were mostly in the range from <0.1-0.6, and in summer samples ranged up to 1.3. Hence the two datasets appear broadly consistent, although the period of ageing of the emissions in the Saudi Arabian air masses is likely to be much smaller, provided the PAH are emitted in the vicinity of Yanbu as Harrison et al. (2016) hypothesise. In the work of Alam et al. (2014) in the UK, ratios of anthraquinone to anthracene (AQ:ANT) in winter were again higher in the more aged air masses mostly in the range of 1.0-1.8. In the less aged air masses winter ratios of AQ:ANT ranged from 0.2-0.7. In summer, in the more aged arctic air, AQ:ANT was generally higher than in the winter with all data in the range of 1.1-1.8 and in the less aged air was 0.2-0.8. In the Saudi Arabian air masses, AQ/ANT was much higher with ratios ranging from 1.2-33.8. The other ratio reported by Alam et al. (2014) was for benzo(a)anthracene-7,12-quinone which showed winter ratios to benzo(a)anthracene from 0.2-1.4 (BaAQ:BaA) with ratios in the more aged air masses generally >1.0, but always <1.0 in the less aged air. Ratios in the Saudi Arabian dataset ranged from <0.1-4.6. From this comparison, we infer that the ratios for PQ:PHE and BaAQ:BaA are broadly comparable in the current dataset from Saudi Arabia to that from the UK reported by Alam et al. (2014).

It is noteworthy that the rate coefficient for oxidation of anthracene by the hydroxyl radical is a factor of 5.1 times greater than that of phenanthrene. Consequently if the processing time were shorter in Saudi Arabia as would be consistent with transport of emissions arising from the Yanbu petrochemical works, but the hydroxyl radical concentrations were greater, then higher AQ:ANT

ratios than PQ:PHE ratios would be expected, and are observed. Due to higher sunlight intensity and hence more rapid ozone photolysis, combined with higher absolute water vapour concentrations in the Saudi atmosphere, higher concentrations of hydroxyl radical are to be expected. At a representative hydroxyl radical concentration of 2×10^6 cm^{-3}, the atmospheric lifetime (time taken to reduce concentration by 1/e) of anthracene is around one hour, whereas that for phenanthrene is around 5.5 hours. The travel time for the air mass from Yanbu to Rayes is of the order of 2-3 hours. It should be remembered that the samples were collected over 24-hour periods and hence include nighttime when reactions will have been much slower than during daytime. Although nocturnal reactions with the NO_3 radical are possible (Keyte et al., 2013), their rate is very uncertain without knowledge of the concentration either of NO_3 itself, or of its precursor NO_2.

3.2 Seasonal Variations in Ratios

Walgraeve et al. (2010) reviewed quinone:parent PAH ratios from various parts of the world, reporting that during winter, 50% of ratios fell between 0.006 and 0.16. On the other hand, in summer, ratios were typically 20-fold higher, with 50% lying between 0.54 and 3.6.

Ratios between quinones and their parent PAH were scrutinised for seasonal differences (see also discussion above). Compounds showing a marked elevation in quinone:PAH ratio in the summer samples were anthraquinone and phenanthraquinone, while ratios for other quinones, acenaphthoquinone to acenaphthene, 2-methylanthraquinone and 2,3-dimethylanthraquinone to anthracene did not show obvious seasonal differences. The quinone:PAH ratio may be viewed as reflecting the relative stability of the parent PAH and quinone to oxidation. The oxidative capacity of the atmosphere is expected to be greater in summer than winter, and those compounds for which quinone/parent PAH ratios are elevated in summer seem likely to be those for which the quinone is more resistant to oxidation than the parent PAH.

Some contrasting behaviour was seen in the nitro-PAH compounds. The compounds 1-nitronaphthalene, 2-nitronaphthalene, 1-nitrofluoranthene, 2-nitrofluoranthene and 1-nitropyrene showed higher concentrations in winter than summer. These compounds include some which arise predominantly from primary emissions and others largely resulting from atmospheric chemical reactions of PAH. The nitro-PAH are subject to atmospheric decay by photolysis (Phousongphouang and Arey, 2003; Feilberg et al., 1999; Reisen and Arey, 2005) and hence it might be expected to find higher concentrations when sunlight is less intense, unless more rapid formation via a photochemically driven pathway outweighs this. Not only were concentrations of nitro-PAH higher in the winter, ratios of 9-nitroanthracene:anthracene, 1-nitrofluoranthene:fluoranthene, 2-nitrofluoranthene:fluoranthene, 1-nitropyrene:pyrene, 2-nitropyrene:pyrene, and 6-nitrochrysene:chrysene, were all higher in the winter samples.

3.3 Spatial Variation of Concentrations

As seen in Figure 2 there was remarkable similarity in the concentrations measured at all three sites for anthraquinone, and phenanthraquinone, and between Rabegh (Site D) and Rayes (Site E) there was quite close agreement for acenaphthoquinone, 2-methyl-anthraquinone, 2,3-dimethylanthraquinone and benzo(a)anthracene-7,12-dione. The Coefficient of Divergence (COD), defined in Harrison at al. (2016) is a measure of spatial uniformity of concentrations. It takes values between zero (total uniformity) and one (totally divergent). In all cases, the COD (see Table 4) was below 0.3, and in the closest case (phenanthraquinone and anthraquinone between Rabegh and Rayes) was <0.1. This level of agreement was much higher than for the PAH concentrations. Also in the case of 1,5-dinitronaphthalene, 9-nitroanthracene, 1-nitrofluoranthene, 2-nitrofluoranthene and 7-nitrobenzo(a)anthracene the COD was <0.3 for Rabegh and Rayes, showing moderate agreement. This high degree of spatial uniformity is typically seen for secondary pollutants such as sulphate, which are formed slowly in the atmosphere, and are subject to sink processes working on a long timescale. Rates of sulphur dioxide oxidation to form sulphate are typically only about 1-3%

per hour, far slower than the comparatively very rapid oxidation processes of the predominantly vapour phase PAH, such as anthracene and phenanthrene. It would appear that the lifetimes of the quinones are far greater than those of the parent PAH, or they would show far greater spatial dependence than is actually observed. Following this line of argument, it appears that the lifetimes of the majority of nitro-PAH would probably be intermediate between those of the PAH (short) and quinones (long). The increase in quinone:PAH ratios with atmospheric transport seen by Alam et al. (2013; 2014) and in this work is consistent with quinones having greater stability than the parent compound.

3.4 Spatial Transformation of PAH and Derivatives

As outlined by Harrison et al. (2016), who show an example trajectory, there were 14 days on which the air mass arriving at Abhur had followed the Red Sea coast from the northwest. As some data were missing, data were averaged for a sub-set of 4 days with complete data, and a coastal trajectory. Figure 2 shows (a) the average PAH, (b) average quinones, and (c) average nitro-PAH concentrations at the three sites over these days. The average travel time of the air mass between sites E (Rayes) and C (Abhur) was estimated as 9.5 hours. Figure 2(a) shows a substantial decline in the concentrations of all PAH, which could be the result of dilution with cleaner air, or chemical reactions, or more probably a combination of the two. The quinones (Figure 2(b)) show much greater spatial uniformity, reflected in low coefficients of divergence (Table 4(a)), probably reflecting their largely secondary nature (although there is an important primary component) and suggesting appreciable longevity. It is clear that the PAH loss between sites seen in Figure 2(a) is not converted to any substantial degree into quinone, or there would be larger inter-site differences seen in Figure 2(b). The nitro-PAH do show greater spatial variation (Figure 2(c) and Table 4(b)). Most nitro-PAH have a primary component, and the spatial differences seen in Figure 2(c) may reflect dilution of primary emitted material. This, however, seems unlikely. If the major upwind source is a petrochemical plant, vapour loss is likely to be the largest PAH source and this would

contain PAH, but not the quinones and nitro-PAH which are combustion products. Consequently, nitro-PAH are more probably reflective of reaction products, and their concentrations reflect a balance between formation and loss, the latter predominantly by photolysis (Phousongphouang and Arey, 2003; Feilberg et al., 1999; Reisen and Arey, 2005).

Ratios between nitrofluoranthene and nitropyrene compounds can be indicative of atmospheric processes. Specifically, the 2-nitrofluoranthene:1-nitropyrene ratio (2-NF/1-NP) is indicative of the relative contribution of atmospheric reactions via OH and NO_3 relative to direct emissions (Keyte et al., 2013). A ratio >5 can be taken as indicative of atmospheric reactions, while a ratio <5 is more likely to reflect direct emissions. Mean site ratios in this study varied between 1.98 at site E and 5.38 at site C (Table 5) indicating contributions from both sources. It is notable that the ratio rises monotonically from site E (Rayes) to site C (Abhur) showing an increasing influence of atmospheric chemical formation. The ratio of 2-nitrofluoranthene:2-nitropyrene (2-NF/2-NP) can be diagnostic of the relative importance of OH and NO_3 radicals in oxidising PAH. A value of between 5-10 indicates dominance of the OH reaction, while those of >100 reflect an important contribution of NO_3 radical attack on the aromatic compound (Keyte et al., 2013). In this study, ratios remained close to 5 (see Table 5), suggesting that the OH radical is the more important reactant. For identical concentrations of fluoranthene and pyrene, the yield ratio for OH reaction is 2-nitrofluoranthene:2-nitropyrene = 6, which is close to our observed values. This is similar to that observed by Alam et al. (2015) in Birmingham, UK.

3.5 Decay Rates of PAH

With the exception of acenaphthene which reacts rapidly with ozone, the atmospheric degradation of PAH is primarily by reaction with the hydroxyl radical (Keyte et al., 2013). Rate coefficients are available for the reaction of the vapour of low molecular weight PAH with the hydroxyl radical, hence allowing prediction of their atmospheric decomposition. The use of such decay rates is

however difficult to relate to decay during transport in the atmosphere since a plume containing PAH will be subject to dilution and potentially to the introduction of fresh emissions. In the case of the three sites to the north of Jeddah (Rayes, Rabegh and Abhur), there are relatively few PAH sources and the possibility exists that the plume from the Yanbu petrochemical works would travel to the southeast with relatively little injection of fresh pollutant. Since PAH react at very different rates with the hydroxyl radical, the ratios between congeners should change in a consistent manner irrespective of absolute concentrations which are affected by dilution processes. The concept was tested by application of the following equation which describes the change of PAH ratios as a function of their relative rates of reaction with the hydroxyl radical:

$$\ln([PAH_i]_t/[PAH_j]_t) = \ln([PAH_i]_0/[PAH_j]_0) + [OH](k'(g)OH - k(g)OH)t$$

where $[PAH_i]_t$ and $[PAH_j]_t$ are the final concentrations of PAH congeners i and j after reaction time (t), $[PAH_i]_0$ and $[PAH_j]_0$ are the initial concentrations of PAH congeners, [OH] is an estimated hydroxyl concentration, and k(g)OH and k'(g)OH are the OH reaction rate coefficients for PAH_i and PAH_j, respectively. It is assumed that the compounds considered in the calculation are wholly in the vapour phase, as only a very small proportion of the low molecular weight compounds is in the condensed phase (Alghamdi et al., 2015 and Table 1). It is also assumed that loss by deposition is similar for both compounds.

The unknown in the equation is the hydroxyl radical concentration which can be output from the calculation, and can be compared with measured or modelled values giving a valuable check on the likelihood that the concentration changes seen are consistent with this reaction.

For periods with appropriate air mass back trajectories, the ratios of PAH congeners (fluorene, phenanthrene, anthracene, fluoranthene and pyrene) were used in the above equation for a source site (Rayes or Rabegh) and a receptor site (Rabegh or Abhur) and a travel time estimated from the air mass back trajectory calculated using HYSPLIT. The results of this calculation were in many

cases inconsistent with the congener ratios changing due solely to reaction with the hydroxyl radical except in the case of 29th September which was the date with the highly elevated concentrations which are shown for the three sites in Figure 3. For this date, the various combinations of sites and congener ratios led to broadly consistent estimates of hydroxyl radical concentration (24-hour mean) and a typical value calculated from concentration of phenanthrene and anthracene at Rayes and Abhur is 3.4×10^5 cm^{-3}. This is low in relation to what might be anticipated as a hydroxyl radical concentration for rural Saudi Arabia based upon published data. Bahm and Khalil (2004) estimate September zonally averaged OH concentrations at 0.5km altitude and 25°N as 2.6×10^6 cm^{-3}. They comment that the Spivakovsky model (Spivakovsky et al., 2000) and MOZART-1 model (Brasseur et al., 1998; Hauglustaine et al., 1998) estimate lower OH over land near the surface. An important consideration, however, is that a release of PAH from the petrochemical works is likely to have been accompanied by much greater concentrations of other volatile organic compounds whose effect on the concentration of hydroxyl radical is difficult to predict as many would act as a sink, although the cycling of OH through peroxy radical chemistry may well also be promoted. This effect cannot be quantified without measurements of concentrations of VOC and NO_x, and a chemistry-transport model, or direct OH measurements.

Our inference is that the concentrations measured on 29th September are consistent with the decay of PAH by reaction with a relatively low concentration of hydroxyl radical; however, data for the other days could not be fitted with this model suggesting that emissions of PAH from intermediate sites on the air mass trajectory introduced fresh pollutant hence changing congener ratios from those which would have prevailed in the absence of such emissions.

The data in Table 1 has been scruitinised to look for any consistent shift in the % particulate which would be indicative of a preferential reaction of either the vapour or condensed phase of the PAH (Keyte et al, 2013). No obvious pattern of behaviour is seen in Table 1 which is unsuprising as PAH

388 repartition actively between the phases in response to changing temperature or concentrations
389 within a phase, in order to restore the phase equilibrium.
390
391 **4. CONCLUSIONS**
392 The spatial distribution of PAH and their nitro- and oxy- derivatives have been demonstrated
393 through sampling at three sites on the Red Sea coast of Saudi Arabia. The PAH show greater
394 spatial variability than either the oxy derivatives (quinones) or nitro-PAH reflecting their greater
395 chemical reactivity. The more abundant quinone compounds show a high degree of spatial
396 uniformity consistent with their presence primarily as secondary pollutants, and the ratio of
397 quinones to parent PAH increases with distance from the probable major source of PAH which is a
398 petrochemical works to the northwest of the sampling locations. The concentrations of PAH decline
399 monotonically from northwest to southeast as air masses travel along the Red Sea coast, which is a
400 result both of chemical degradation and atmospheric dilution. The influence of chemical reactions
401 has been assessed through the evaluation of changing ratios of compounds of different reactivity,
402 which inherently controls for concentration changes due to dilution. Using the assumption that the
403 breakdown of PAH is due to the reaction with hydroxyl radical, concentrations of hydroxyl have
404 been calculated from the changing PAH ratios and estimated travel time of air masses between the
405 sampling sites. In general the calculations do not yield realistic values for OH except for one day,
406 29th September 2013, when higher PAH concentrations were observed. However the calculated OH
407 radical concentration is significantly lower than the prediction of global models, which maybe due
408 to emissions of VOC and NO_x acting as a sink for OH or may be due to other sources of PAH
409 emissions influencing concentrations between the source and receptor sites. However the results
410 illustrate that atmospheric transport of PAH across a sparsely populated desert area is accompanied
411 by an atmospheric breakdown rate broadly consistent with anticipated free radical concentrations.
412 On other days, it appears likely that PAH emitted between the upwind and downwind sites has a
413 sufficient influence upon the ratio to make the calculation unworkable.

5. ACKNOWLEDGEMENTS

Authors are indebted for financial support by Saudi Ministry of Higher Education and Deanship of Scientific Research (DSR) at King Abdulaziz University. This work was funded with a grant #2/H/1434.

REFERENCES

Alam, M.S., Delgado-Saborit, J.M., Stark, C., Harrison, R.M., 2013. Using atmospheric measurements of PAH and quinone compounds at roadside and urban background sites to assess sources and reactivity. Atmos. Environ. 77, 24-35.

Alam, M.S., Delgado-Saborit, J.M., Stark, C., Harrison, R.M., 2014. Investigating PAH relative reactivity using congener profiles, quinone measurements and back trajectories. Atmos. Chem. Phys. 14, 2467-2477.

Alam, M.S., Keyte, I.J., Yin, J., Stark, C., Jones, A.M., Harrison, R.M., 2015. Diurnal variability of polycyclic aromatic compound (PAC) concentrations: Relationship with meteorological conditions and inferred sources. Atmos. Environ. 122, 427-438.

Albinet, A., Leoz-Garziandia, E., Budzinski, H., ViIlenave, E., 2006. Simultaneous analysis of oxygenated and nitrated polycyclic aromatic hydrocarbons on standard reference material 1649a (urban dust) and on natural ambient air samples by gas chromatography-mass spectrometry with negative ion chemical ionisation. J. Chromat. A. 1121, 106-113.

Albinet, A., Leoz-Garziandia E., Budzinski, H., Villenave, E., 2007. Polycyclic aromatic hydrocarbons (PAHs), nitrated PAHs and oxygenated PAHs in ambient air of the Marseilles area (South France): Concentrations and sources. Sci. Total Environ. 384, 280-292.

Albinet, A., Leoz-Garziandia, E., Budzinski, H., Villenave, E., Jaffrezo, J.L., 2008. Nitrated and oxygenated derivatives of polycyclic aromatic hydrocarbons in the ambient air of two French alpine valleys – part 1: concentrations, sources and gas/particle partitioning. Atmos. Environ. 42, 43-54

Alghamdi, M.A., Alam, M.S., Yin, J., Stark, C., Jang, E., Harrison, R.M., Shamy, M., Khoder, M.I., Shabbaj, I.I., 2015. Receptor modelling study of polycyclic aromatic hydrocarbons in Jeddah, Saudi Arabia. Sci. Tot. Environ. 506-507, 401-408.

Bahm, D., Khalil, M.A.K., 2004. A new model of tropospheric hydroxyl radical concentrations. Chemosphere 54, 143-166.

Brasseur, G.P., Hauglustaine, D.A., Walters, S., Rasch, P.J., Muller, J.-F., Grainer, C., Tie, X.X., 1998. MOZART, a global chemical transport model for ozone and related chemical tracers. 1. Model description. J. Geophys. Res 103, 28265-28289.

Cochran, R.E., Dongari, N., Jeong, H., Beranek, J., Haddadi, S., Shipp, J., Kubatova, A., 2012. Determination of polycyclic aromatic hydrocarbons and their oxy-, nitro-, and hydroxy-oxidation products. Analytica Chimica Acta. 740, 93-103.

Delgado-Saborit, J.M., Aquilina, N., Baker, S., Harrad, S., Meddings, C., Harrison, R.M., 2010. Determination of atmospheric particulate-phase polycyclic aromatic hydrocarbons from low volume air samples. Anal. Methods 2, 231-242.

Delgado-Saborit, J.M., Alam, M.S., Godri, K.J., Stark, C., Harrison, R.M., 2013. Analysis of atmospheric concentrations of quinones and polycyclic aromatic hydrocarbons in vapour and particulate phases. Atmos. Environ. 77, 974-982.

Dimashki, M., Harrad, S., Harrison, R.M., 2000. Measurement of nitro-PAH in the atmospheres of two cities. Atmos. Environ. 34, 2459-2469.

Durant, J.L., Busby Jr, W.F., Lafleur, A.L., Penman, B.W., Crespi, C.L., 1996. Human cell mutagenicity of oxygenated, nitrated and unsubstituted polycyclic aromatic hydrocarbons associated with urban aerosols. Mutat. Res. 123-157.

Feilberg, A., Kamens, R.M., Strommen, M.R., Nielsen, T., 1999. Photochemistry and partitioning of semivolatile nitro-PAH in the atmosphere. Polycycl. Aromat. Comp. 14 & 15, 151-160.

Harrison, R.M., Smith, D.J.T. and Luhana, L. 1996. Source apportionment of atmospheric polycyclic aromatic hydrocarbons collected from an urban location in Birmingham, UK, Environ. Sci. Technol. 30, 825-832.

Harrison, R.M., Alam, M.S., Dang, J., Basahi, J., Alghamdi, M.A., Ismail, I.M., Khoder, M., Hassan, I.A., 2016. Influence of petrochemical installations upon PAH concentrations at sites in western Saudi Arabia. Atmos. Pollut. Res. in press.

Hauglustaine, D.A., Brasseur, G.P., Walters, S., Rasch, P.J., Muller, J.-F., Emmons, L.K., Carroll, M.A., 1998. MOZART, a global chemical transport model for ozone and related chemical tracers. 2. Model results and evaluatin. J. Geophys. Res. 103, 28291-28335.

Keyte, I.J., Harrison, R.M. and Lammel, G., 2013. Chemical reactivity and long-range transport potential of polycyclic aromatic hydrocarbons - A review. Chem. Soc. Rev. 42, 9333-9391.

Li, N., Sioutas, C., Cho, A., Schmitz, D., Misra, C., Sempf, J., Wang, M., Oberley, T., Froines, H., Nel, A., 2003. Ultrafine particulate pollutants induce oxidative stress and mitochondrial damage. Environ. Health Perspect. 111, 455.

Pederson, T.C., Siak, J.-S., 1981. The role of nitroaromatic compound sin the direct-acting mutagenicity of diesel particle extracts. J. Appl. Toxicol. 1, 54-60.

Phousongphouang, P.T., Arey, J., 2003. Rate constants for the photolysis of the nitroaphthalenes and methylnitronaphthalenes. J. Photochem. Photobiol. A: Chemistry 157, 301-309.

Ravindra, K., Sokhi, R. and Van Grieken, R., 2008. Atmospheric polycyclic aromatic hydrocarbons: Source attribution, emission factors and regulation. Atmos. Environ. 42, 2895-2921.

Reisen, F., Arey, J., 2005. Atmospheric reactions influence seasonal PAH and Nitro-PAH concentrations in the Los Angeles Basin. Environ. Sci. Technol. 39, 64-73.

Ringuet, J., Leoz-Garziandia, E., Budzinski, H., Villenave E., Albinet A., 2012. Particle size distribution of nitrated and oxygenated polycyclic aromatic hydrocarbons (NPAHs and OPAHs) on traffic and suburban sites of a European megacity: Paris (France). Atmos. Chem. Phys. 12, 8877-8887.

Souza, K.F., Carvalho, L.R.F., Allen, A.G., Cardoso, A.A., 2014. Diurnal and nocturnal measurements of PAH, nitro-PAH, and oxy-PAH compounds in atmospheric particulate matter of a sugar cane burning region. Atmos. Environ. 83, 193-201.

Spivakovsky, C.M., Logan J.A., Montzka, S.A., Balkanski, Y.J., Foreman-Fowler, M., Jones, D.B.A., Horowitz L.W., Fusco, A.C., Brenninkmeijer, C.A.M., Prather, M.J., Wofsy, S.C., McElroy, M.B., 2000. Three-dimensional climatological distribution of tropospheric OH: Update and evaluation. J. Geophys, Res. 105, 8931-8980.

Verma, V., Wang, Y., El-Afifi, R., Fang, T., Rowland, J., Russell, A.G., Weber, R.J., 2015. Fractionating ambient humic-like substances (HULIS) for their reactive oxygen secies activity – Assessing the importance of quonones and atmospheric aging. Atmos. Environ. 120, 351-359.

Walgraeve, C., Demeestere, D., Dewulf, J., Zimmermann, R., Van Langenhove, H., 2010. Oxygenated polycyclic aromatic hydrocarbons in atmospheric particulate matter: molecular characterization and occurrence. Atmos. Environ. 44, 1831-1846.

WHO, 2010. WHO Guidelines for Indoor Air Quality: Selected Pollutants, World Health Organization, Regional Office for Europe, Copenhagen, Denmark.

TABLE CAPTIONS

Table 1: Total concentrations of PAH, quinones, and nitro-PAH compounds and percentage in the particulate phase at Abhur (site C), Rabegh (site D) and Rayes (site E) (ng m^{-3}).

Table 2: Range of concentrations of PAH quinones reported in the literature.

Table 3: Range of concentrations of nitro-PAH reported in the literature.

Table 4: Coefficients of Divergence (COD) values for (a) oxy-PAHs; (b) nitro-PAHs.

Table 5: Range and mean of ratios at C (Abhur), D (Rabegh) and E (Rayes) sties for nitrofluoranthene and nitropyrene isomers.

FIGURE CAPTIONS

Figure 1: Locations of sampling sites and the city of Jeddah. The sites are: C Abhur; D-Rabegh and E-Rayes. Sites A and B are within Jeddah.

Figure 2: Figure 2: (a) Total PAH; (b) total oxy-PAH and (c)total nitro-PAH averaged over 4 days on which the air travelled from northwest to southeast following the Red Sea coast.

Figure 3: (a) Total PAH, (b) total oxy-PAH and (c) total nitro-PAH at the three sites on 29th September 2013.

Table 1: Total concentrations of PAH, quinone, and nitro-PAH compounds and percentage in the particulate phase at Abhur (site C), Rabegh (site D) and Rayes (site E) (ng m^{-3}).

PAH Congener	Site C				Site D				Site E			
	Mean	Range	Number of samples	Mean P%	Mean	Range	Number of samples	Mean P%	Mean	Range	Number of samples	Mean P%
Fluorene	0.47	0.20-1.54	10	1.8%	0.91	0.45-1.92	15	0.7%	1.13	0.36-6.98	22	0.9%
Phenanthrene	6.03	2.57-12.09	10	3.1%	7.74	4.51-14.41	15	2.0%	9.58	3.24-29.92	22	1.9%
Anthracene	0.31	0.14-0.79	10	4.5%	0.40	0.20-1.30	15	2.8%	0.82	0.19-7.53	22	2.4%
Fluoranthene	0.94	0.50-1.67	10	6.3%	1.20	0.69-2.53	15	4.5%	1.18	0.40-5.86	22	5.9%
Pyrene	0.89	0.43-1.50	10	7.5%	1.44	0.79-2.51	15	3.9%	1.11	0.27-7.08	22	7.2%
Retene	0.56	0.05-1.14	10	16.0%	0.49	0.16-1.09	15	5.3%	0.52	0.21-1.75	22	8.6%
Benzo(a)anthracene	0.26	0.05-0.59	10	27.6%	0.39	0.04-1.00	15	21.0%	0.37	0.02-1.48	22	30.0%
Chrysene	0.26	0.07-0.47	10	60.4%	0.30	0.02-0.61	15	54.4%	0.39	0.06-1.91	22	47.7%
Benzo(b)fluoranthene	0.12	0.01-0.25	19	88.1%	0.16	0.05-0.25	22	85.8%	0.23	0.04-1.53	22	78.2%
Benzo(k)fluoranthene	0.12	0.02-0.23	19	90.3%	0.16	0.02-0.25	22	86.5%	0.24	0.04-2.08	22	84.7%
Benzo(e)pyrene	0.10	0.01-0.27	19	100.0%	0.11	0.02-0.29	22	100.0%	0.19	0.03-1.68	22	100.0%
Benzo(a)pyrene	0.07	0.01-0.16	19	100.0%	0.09	0.01-0.14	22	100.0%	0.16	0.01-1.53	22	100.0%
Indeno(1,2,3-cd)pyrene	0.09	0.01-0.17	19	100.0%	0.09	0.02-0.29	22	100.0%	0.18	0.03-1.89	22	100.0%
Dibenz(a,h)anthracene	0.03	0.01-0.08	19	100.0%	0.04	0.01-0.12	22	100.0%	0.08	0.01-0.67	22	100.0%
Benzo(ghi)perylene	0.11	0.02-0.32	19	100.0%	0.18	0.04-0.69	22	100.0%	0.24	0.04-2.32	22	100.0%
Coronene	0.09	0.03-0.21	19	100.0%	0.16	0.04-0.45	22	100.0%	0.20	0.06-1.54	22	100.0%
Quinone Congener												
1,4-Naphthoquinone	0.00	0.00-0.01	19	100.0%	n.d.	n.d.	22	n.d.	n.d.	n.d.	22	n.d.
2-Methyl-1,4-naphthoquinone	0.12	0.02-0.41	19	100.0%	0.10	0.05-0.14	22	100.0%	0.11	0.01-0.26	22	100.0%
Acenaphthoquinone	9.14	1.70-23.30	10	0.2%	10.89	2.44-25.62	15	9.6%	6.61	2.84-11.31	22	12.6%
Anthraquinone	3.31	0.44-8.37	10	3.9%	4.02	0.80-9.33	15	19.0%	3.15	0.76-8.92	22	16.9%
Phenanthraquinone	2.31	0.31-5.93	10	5.7%	2.86	0.57-7.35	15	18.6%	2.34	0.52-8.25	22	16.4%
2,6-Di-tert-butyl-1,4-benzoquinone	1.43	0.91-2.32	10	6.8%	1.99	1.19-4.74	15	28.5%	1.78	0.71-3.54	22	27.7%
2-Methyl-anthraquinone	0.17	0.05-0.81	10	44.6%	0.52	0.13-0.82	15	81.4%	0.42	0.07-0.93	22	79.8%
2,3-Dimethyl-anthraquinone	0.18	0.12-0.27	10	80.2%	0.38	0.14-0.64	15	91.8%	0.36	0.10-0.80	22	91.9%

Benz(a)anthracene-7,12-dione	0.11	0.01-0.20	19	100.0%	0.05	0.01-0.11	22	100.0%	0.07	0.02-0.37	22	100.0%
5,12-Naphthacenequinone	0.11	0.02-0.20	19	100.0%	0.07	0.01-0.41	22	100.0%	0.09	0.00-0.42	22	100.0%
NPAH Congener												
1-Nitronaphthalene	5.62	1.55-18.82	10	2.0%	6.70	1.43-23.13	15	1.2%	3.98	0.45-13.84	22	2.0%
2-Nitronaphthalene	4.88	1.37-15.65	10	6.6%	4.77	1.60-15.39	15	4.8%	2.41	0.33-7.03	22	5.8%
1,5-Dinitronaphthalene	0.78	0.26-1.57	10	50.9%	0.82	0.44-1.63	15	47.4%	1.07	0.58-1.79	22	52.5%
9-Nitroanthracene	0.61	0.35-1.11	10	56.7%	0.56	0.21-1.08	15	56.0%	0.65	0.24-1.71	22	56.2%
1-Nitrofluoranthene	0.13	0.01-0.57	19	91.7%	0.15	0.02-0.50	22	93.0%	0.23	0.08-0.54	22	91.7%
2-Nitrofluoranthene	0.78	0.13-2.39	19	86.0%	0.50	0.12-1.27	22	89.2%	0.59	0.08-3.32	22	88.5%
1-Nitropyrene	0.34	0.01-2.03	19	89.0%	0.55	0.01-4.23	22	87.5%	0.61	0.06-4.24	22	89.9%
2-Nitropyrene	0.16	0.02-0.44	19	88.6%	0.13	0.02-0.61	22	91.9%	0.23	0.03-1.71	22	93.7%
7-Nitrobenzo(a)anthracene	0.56	0.01-2.49	19	100.0%	0.47	0.10-1.32	22	100.0%	0.53	0.10-1.85	22	100.0%
6-Nitrochrysene	0.06	0.01-0.16	19	100.0%	0.06	0.01-0.19	22	100.0%	0.1	0.01-0.19	22	100.0%

n.d. = not determined

Table 2: Range of concentrations of PAH quinones reported in the literature.

Compound	Concentration (ng m^{-3})
9,10 phenanthrenequinone	0.01 – 2.0
5,12-naphthacenequinone	0.02 – 1.6
1-acenaphthenone	0.01 – 0.45
1,4-naphthoquinone	0.02 – 1.03
Anthracene-9,10-dione	0.056 – 13
2-methylanthraquinone	0.05 – 1.31
Benz(a)anthracene-7,12-dione	0.012 – 1.0
2,3-dimethylanthraquinone	0.04 – 0.54

Table 3: Range of concentrations of nitro-PAH reported in the literature.

Compound	Concentration (pg m^{-3})
1-Nitronaphthalene	0.2 - 700
2-Nitronaphthalene	0.0 - 292
1,5-Dinitronaphthalene	No data
2-Nitrofluorene	0 – 100
9-Nitroanthracene	9 – 846
1-Nitrofluoranthene	0.01 – 0.19[+]
2-Nitrofluoranthene	11.7 – 1700
3-Nitrofluoranthene	0.28 - 250
4-Nitropyrene	0 – 2.9
1-Nitropyrene	1 – 222
7-Nitrobenz(a)anthracene	0.7 – 130
6-Nitrochrysene	0.1 – 148
2-Nitropyrene	0.8 – 60
1,3-Dinitropyrene	0.1 – 1.2
1,6-Dinitropyrene	0 – 0.1
1,8-Dinitropyrene	0.3 – 8.7

[+] Sum of particulate plus vapour phases

Table 4: Coefficients of divergence (COD) values for (a) oxy-PAHs; (b) nitro-PAHs.

(a)			
Species	$COD_{A\&Rg}$	$COD_{A\&Rs}$	$COD_{Rg\&Rs}$
1,4-Naphthoquinone	1.000	0.964	/
2-Methyl-1,4-naphthoquinone	0.349	0.444	0.294
Acenaphthoquinone	0.257	0.224	0.255
Anthraquinone	0.195	0.177	0.101
Phenanthraquinone	0.195	0.185	0.098
2,6-Di-tert-butyl-1,4-benzoquinone	0.270	0.247	0.134
2-Methyl-anthraquinone	0.628	0.575	0.216
2,3-Dimethyl-anthraquinone	0.409	0.425	0.168
Benz(a)anthracene-7,12-dione	0.446	0.377	0.250
5,12-Naphthacenequinone	0.441	0.435	0.343

(b)			
Species	$COD_{A\&Rg}$	$COD_{A\&Rs}$	$COD_{Rg\&Rs}$
1-Nitronaphthalene	0.260	0.415	0.381
2-Nitronaphthalene	0.292	0.480	0.422
1,5-Dinitronaphthalene	0.219	0.332	0.226
9-Nitroanthracene	0.135	0.145	0.156
1-Nitrofluoranthene	0.337	0.457	0.335
2-Nitrofluoranthene	0.302	0.450	0.328
1-Nitropyrene	0.309	0.519	0.421
2-Nitropyrene	0.365	0.471	0.404
7-Nitrobenzo(a)anthracene	0.392	0.396	0.291
6-Nitrochrysene	0.299	0.465	0.451

Note: A = Abhur ; Rg = Rabegh ; Rs = Rayes

Table 5: Range and mean of ratios at C (Abhur), D (Rabegh) and E (Rayes) sites for nitrofluoranthene (NF) and nitropyrene (NP) isomers.

Ratios	Site C		Site D		Site E	
	Mean	**Range**	**Mean**	**Range**	**Mean**	**Range**
2-NF/1-NP	5.38	0.16-11.18	2.82	0.07-9.38	1.98	0.08-6.56
2-NF/2-NP	4.78	2.11-7.40	4.49	1.02-9.19	3.91	0.94-14.12

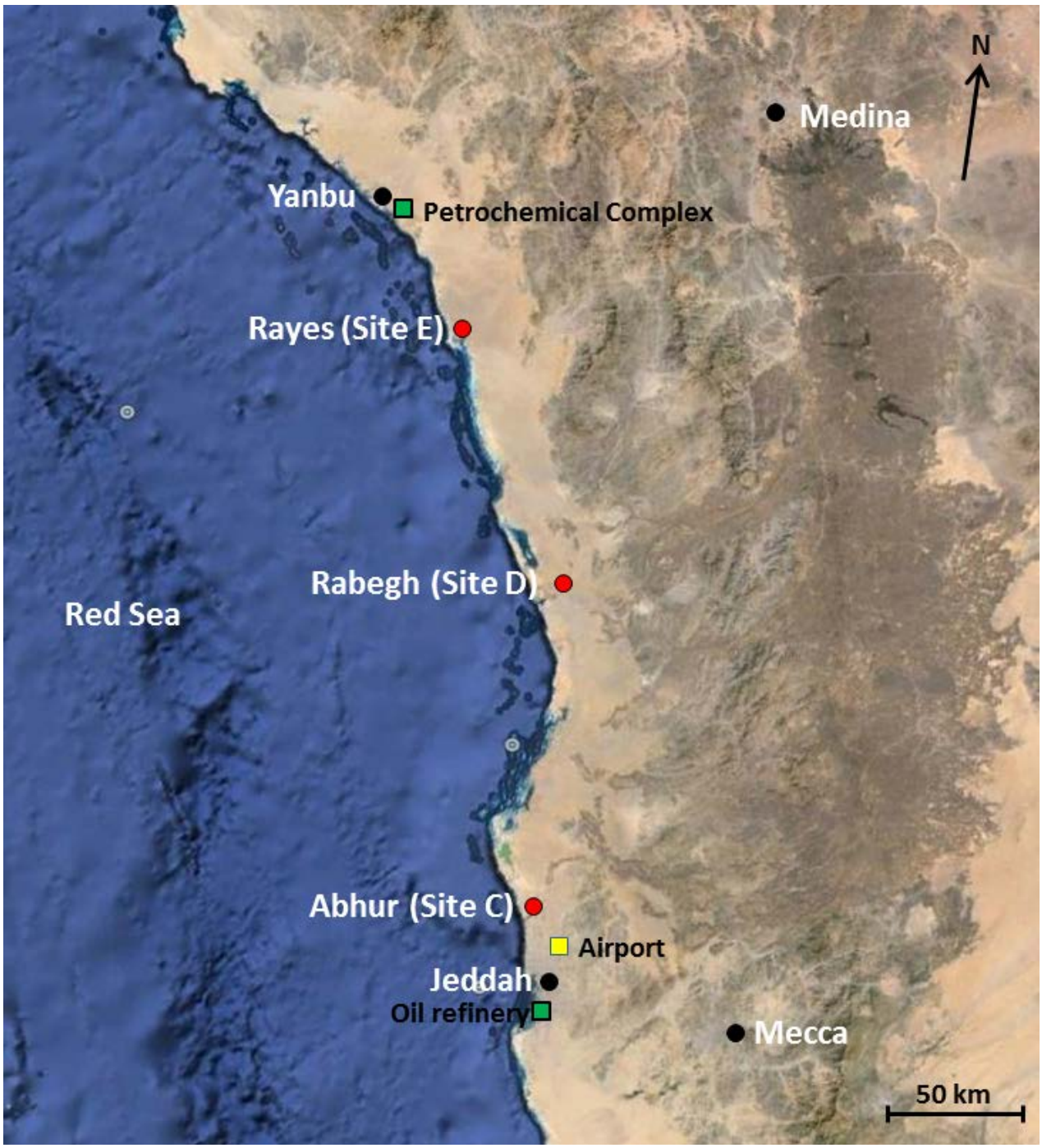

Figure 1: Locations of sampling sites and the city of Jeddah. The sites are: C Abhur; D-Rabegh and E-Rayes. Sites A and B are within Jeddah.

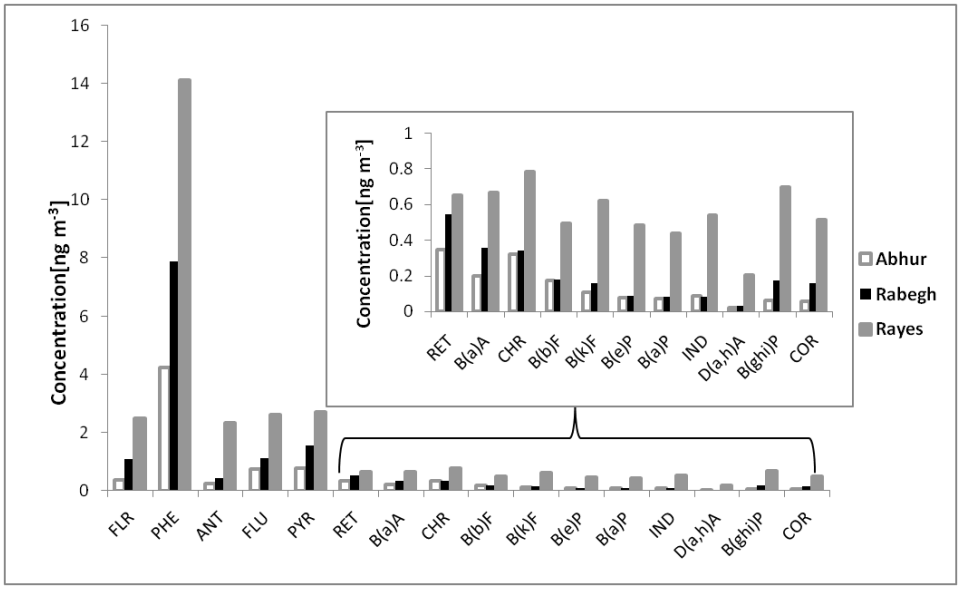

(a)

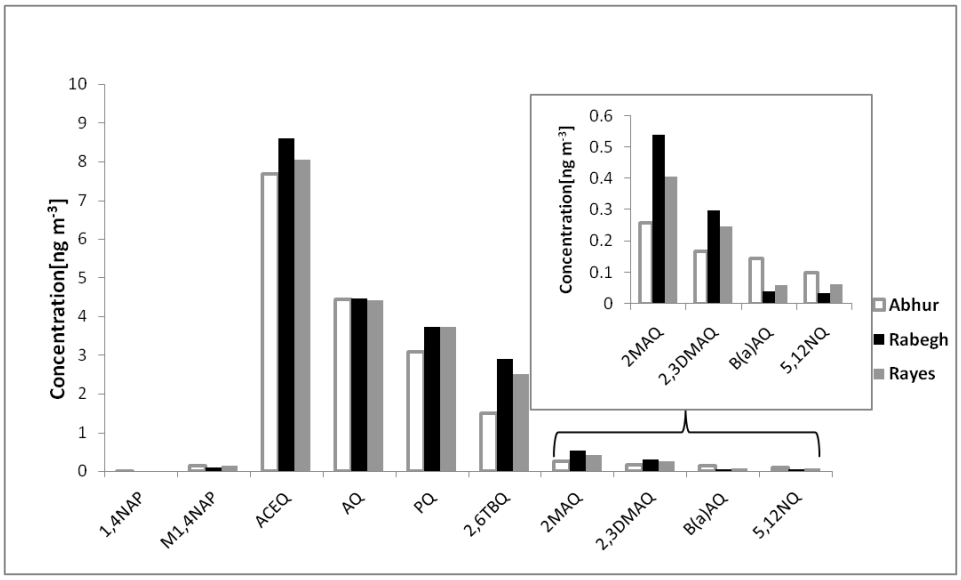

(b)

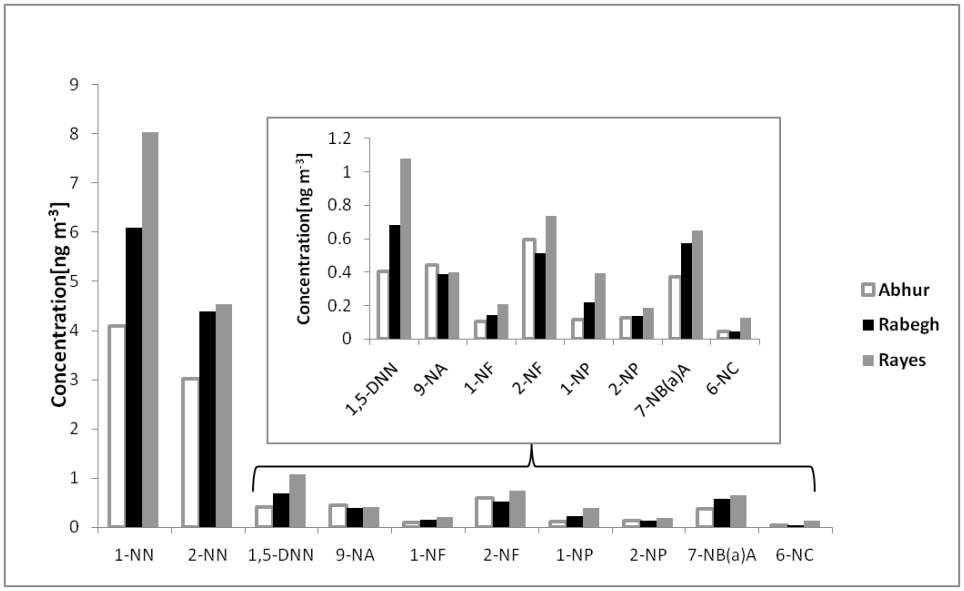

(c)

Figure 2: (a) Total PAH; (b) total oxy-PAH and (c)total nitro-PAH averaged over 4 days on which the air travelled from northwest to southeast following the Red Sea coast.

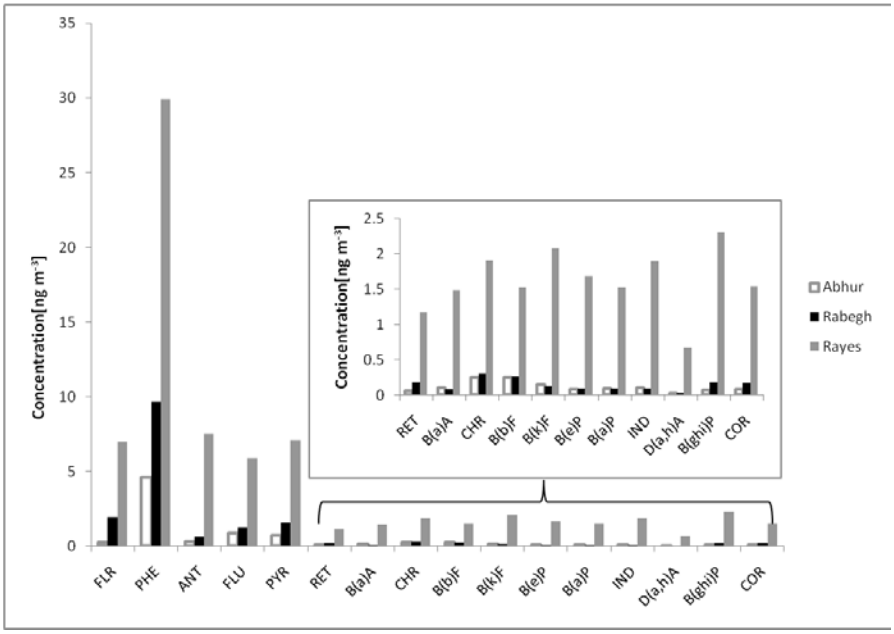

(a)

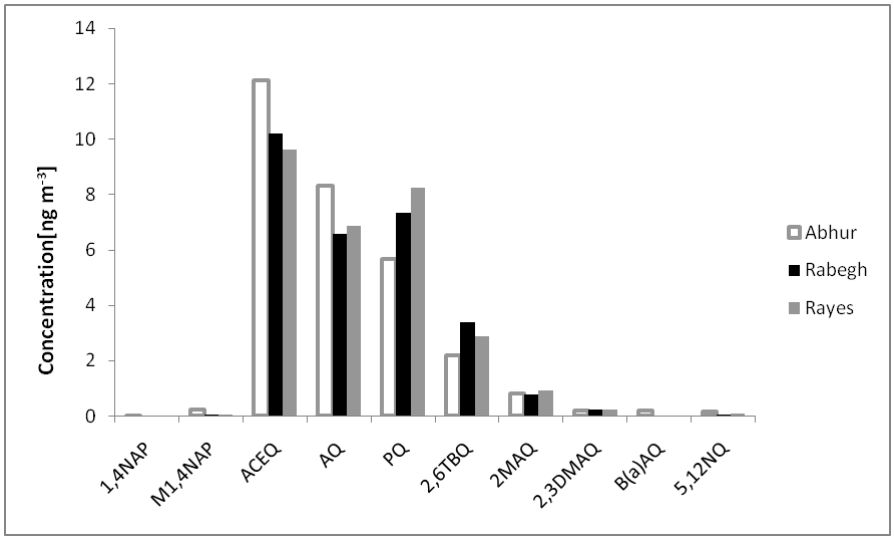

(b)

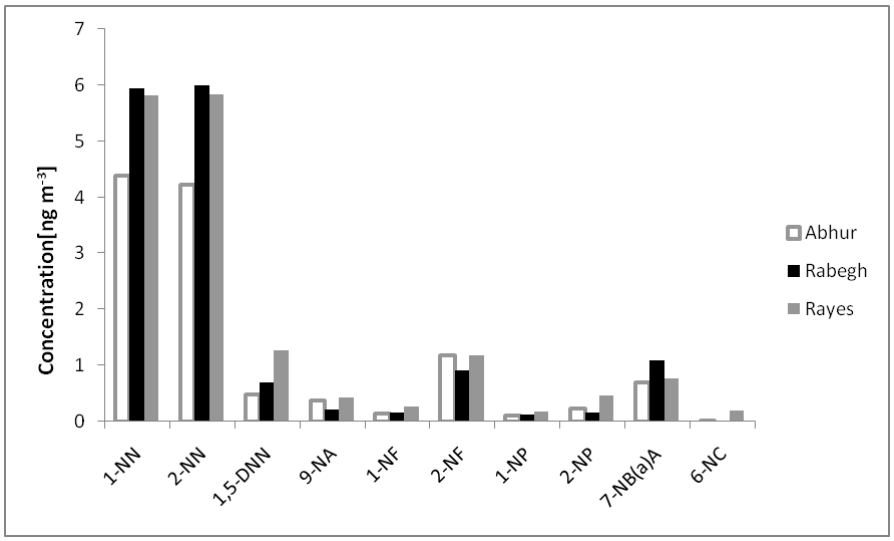

(c)

Figure 3: (a) Total PAH, (b) total oxy-PAH and (c) total nitro-PAH at the three sites on 29th September 2013.